

Spatial Distribution Analyses of Superconducting Transition Temperature in Epitaxial $\text{YBa}_2\text{Cu}_3\text{O}_7$ Film Using Variable Temperature Scanning Laser Microscopy

S. Seo and C. Kwon

Department of Physics and Astronomy, California State University-Long Beach,
Long Beach, CA 90840, U.S.A.

B.H. Park and Q.X. Jia

Superconductivity Technology Center, Los Alamos National Laboratory,
Los Alamos, NM 87545, USA

ABSTRACT

The spatial distribution of superconducting properties using variable temperature scanning laser microscope (VTSLM) has been investigated. The superconducting thin film used in this study is an epitaxial $\text{YBa}_2\text{Cu}_3\text{O}_7$ film photolithographically patterned to a 300 μm -wide bridge. Since the voltage response, $\delta V(x,y)$ is proportional to $dR/dT(x,y)$, the spatial distribution of superconducting transition can be obtained in VTSLM images. In the resistive transition region, there is a strong correlation between the VTSLM images and the resistance of the sample. With decreasing resistance, the area with large $\delta V(x,y)$ shifts toward the ends of the bridge. This indicates that the resistive transition is not uniform and both ends of the bridge have lower transition temperature, T_c . Different currents or different output power of lasers do not affect the images. VTSLM technique is a powerful tool to image the local superconducting properties and to identify the weaker superconducting areas.

INTRODUCTION

Since the discovery to superconductivity in cuprate oxides, a tremendous amount of research has been devoted at fabricating new higher T_c materials, understanding the fundamental properties of these materials, and developing various power and device applications. The complicated crystal structure of high T_c superconductors (HTS) leads to their substantial spatial inhomogeneity, which is especially important because of the very short coherence length in those materials. Consequently, spatially resolved studies of HTS are very effective both to evaluate the general quality of the samples and to determine local values of important parameters. In conventional transport measurements of superconducting samples, the measured quantities such as critical current densities and critical temperatures are averaged over the whole sample and do not reflect the local distribution of the quantities. Thus, spatially resolved studies of HTS are needed to determine local values of important parameters of the samples. Recently, MO imaging technique has been successfully employed to study the flux penetration on coated conductors [1,2]. Another technique is Hall-probe magnetometry using Hall probe arrays to map the local magnetic field distribution [3]. Scanning tunneling microscopy and spectroscopy were also employed to study the spatial variation of superconductivity with nanometer resolution [4]. More direct measurement techniques to study local variations of superconducting properties in HTS are the hot-spot scanning method such as low temperature scanning electron microscopy (LTSEM) and low temperature scanning laser microscopy (LTSLM). In LTSEM experiments, a dc current biased sample is scanned with the electron beam causing a local perturbation at the

point (x, y) of the beam focus. The perturbation can be treated in good approximation as a local heating effect. LTSLM uses a focused laser beam as a heating source. The detected voltage signal $\delta V(x, y)$ yields information about critical temperatures $T_{co}(x, y)$, transition width $\Delta T_c(x, y)$, and critical current densities $j_c(x, y)$ [5]. The comparison of LTSEM and LTSLM images demonstrate that the two techniques produce equivalent images of I_c and T_c [6]; however, due to its inherent insensitivity to magnetic fields, the laser scanning method appears to be preferable for high current applications.

SETUP AND EXPERIMENTS

The VTSLM uses a Helium-Neon laser (632.8 nm) which is modulated at a frequency, f_m , using a standard mechanical chopper (Stanford Research Systems SR540). The laser beam is coupled into an optical fiber, and on the other end, we used a microscope objective lens to focus the beam on the sample. The fiber and the lens are fastened to a 3-axis movable stage system that scans the beam across the sample in both horizontal and vertical directions while simultaneously gathering the ac voltage (with f_m) created by the optical response of the sample using a lock-in amplifier (Stanford Research Systems SR530). The setup is shown in figure 1. The VTSLM method detects AC voltage response δV of a sample biased with a DC current of 0.1 mA-8.0 mA using the current source (Keithley 220) to a local heating by a laser beam chopped with a frequency of about 1.0 kHz.

Measurement of the Beam Diameter

The diameter of the laser beam was investigated using a 20 mW power of HeNe laser and the optic fiber with the diameter of 50 μm . The sample stage was replaced by a razor blade and a screen was put behind the blade. Using a micrometer, the blade can be moved up or down. When the blade starts blocking the beam, it creates a shadow at the edge of the beam image on the screen. When the blade blocks the beam completely, there is no beam image on the screen. A beam diameter can be estimated from the difference between two blade positions, that is,

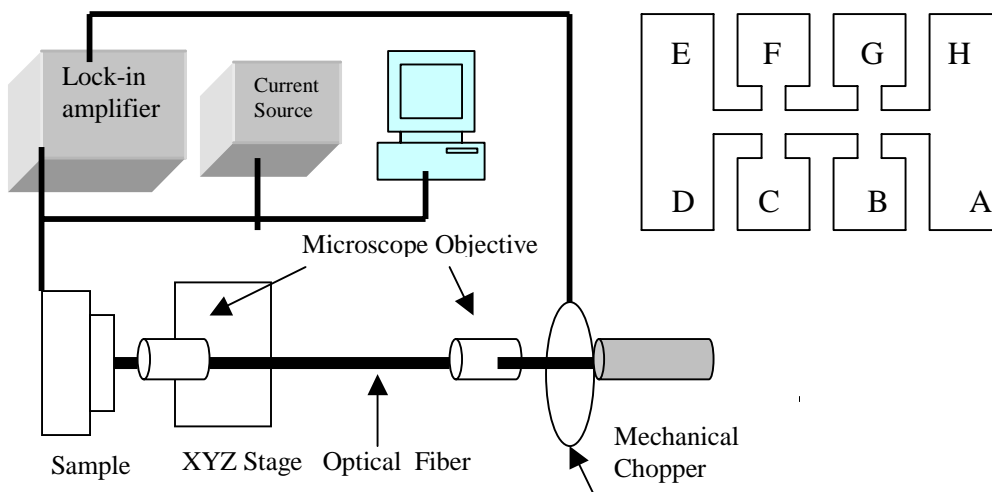


Figure 1. Sketch of the VTSLM setup and Sample Configuration

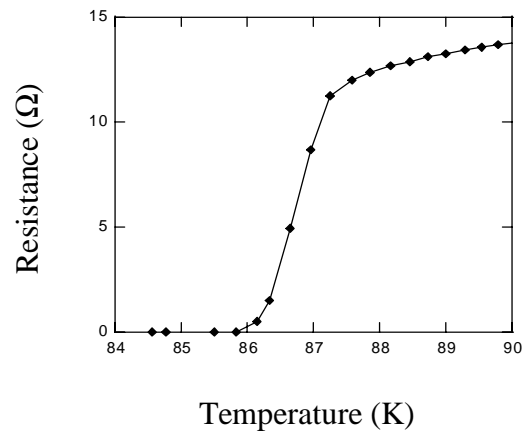
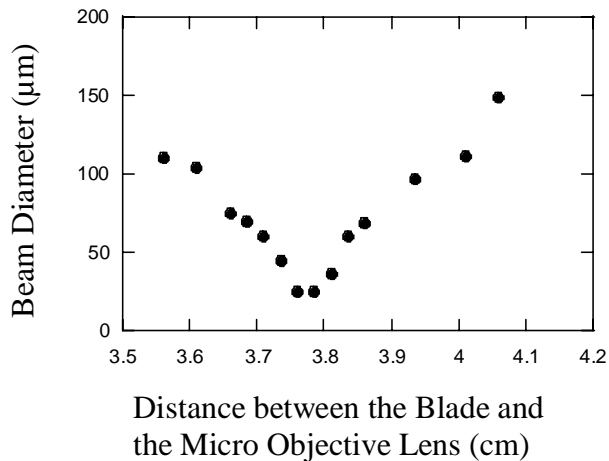


Figure 2. Measurements of the beam diameter. **Figure 3.** Resistance Versus Temperature

once the image starts showing and disappearing. Figure 2 presents the beam diameter versus the distance between the blade and the microscope objective lens using a microscope optic lens with magnification of 10x. The minimum beam diameter of the beam is 24.87 μm. Hence, the sample was laid 3.785 cm away from the microscope objective.

RESULTS

Resistance Versus Temperature

Figure 3 shows the resistance versus temperature with a superconducting transition temperature T_c ($R=0$) of 86.14 K and with a temperature coefficient of resistance (dR/dT) of 10.13 Ω/K at the transition region. To carry the measurements, the bias current of 1.0 μA was applied to the leads E and F separated by 2.0 mm. The voltage was measured between the leads C and D. The sample investigated by VTSLM was a single crystalline $YBa_2Cu_3O_7$ on a $LaAlO_3$ substrate and it has been photo-lithographically patterned to a 300 μm-wide bridge.

AC Voltage Response Line Scans and VTSLM Images

Figure 4(a) shows line scans by measuring AC voltage response at different resistances of (a) 11.800 Ω, (b) 8.595 Ω, (c) 6.430 Ω, and (d) 4.015 Ω with a bias current of 5 mA. Based on the resistance versus the temperature curve shown in figure 3, if the temperature is changed, the resistance is also changed. All of the images were taken at the transition region. A temperature coefficient of resistance (dR/dT) at each resistance was (a) 2.69 Ω/K, (b) 9.92 Ω/K, (c) 10.40 Ω/K and (d) 35.0 Ω/K. It should be mentioned that the magnitude of AC voltage response (δV) and the resistive regions vary with different resistances. For the highest resistance, 11.80 Ω, the response signal was very small compared to those from lower resistance. What is interesting is that the area with large voltage response shifts towards the ends of the bridge with decreasing resistance. Since the beam-induced voltage is generally expected only if

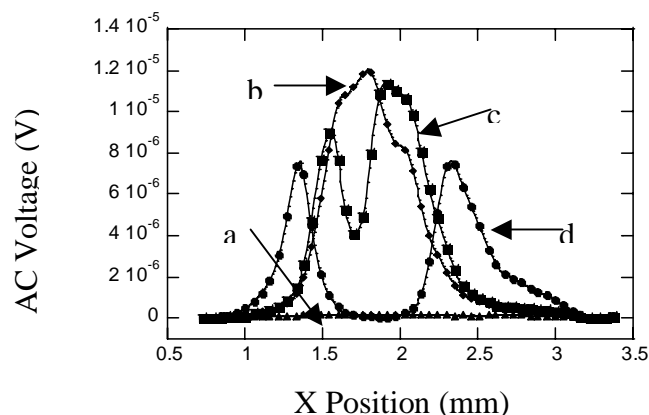


Figure 4. AC voltage response from line scans. (a) 11.80 Ω (b) 8.595 Ω (c) 6.430 Ω (d) 4.015 Ω

the beam is focused on a resistive area that has a larger ac voltage response, figure 4 indicates that the resistive transition region shifts towards the ends with decreasing resistance.

Figure 5 shows the corresponding VTSLM images to figure 4. Bright regions represent high ac voltage response. It is clear that the superconducting transition region moved to the ends of the bridge with decreasing temperature. With decreasing temperature, the middle section of the bridge exhibited a superconducting transition first, as temperature was decreased the superconducting region moved toward the ends of the bridge. We therefore conclude that the ends of the bridge are the weakest regions in that they have the lowest superconducting transition temperature.

VTSLM Images For Different Bias Currents

Figure 6 presents the VTSLM images using three different bias currents less than the critical current, I_c . All of them were taken at the same temperature of the transition region and

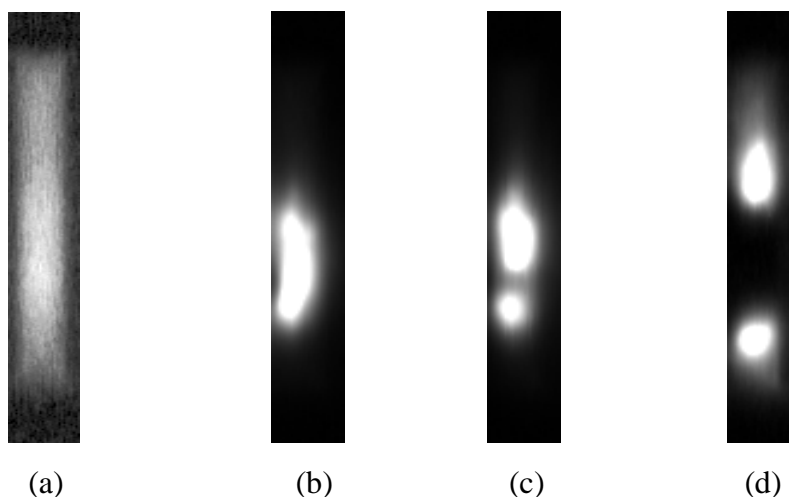


Figure 5. VTSLM Images corresponding to figure 4. (a) 11.80 Ω (b) 8.595 Ω (c) 6.430 Ω (d) 4.015 Ω

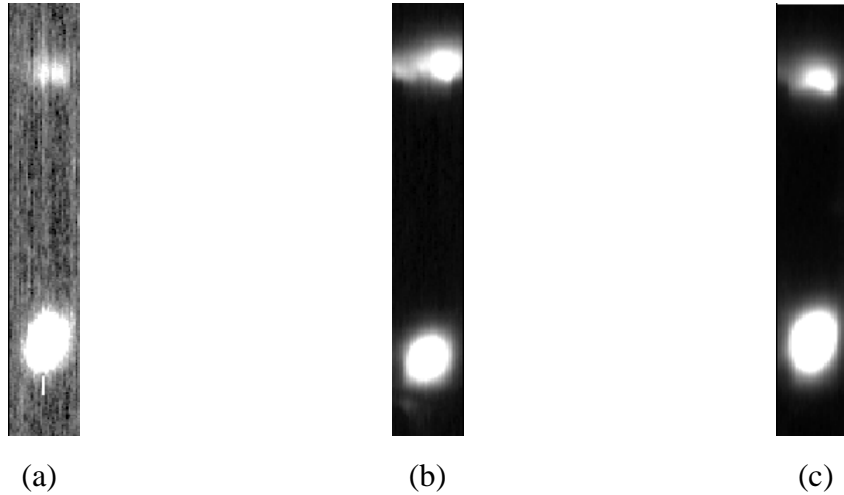


Figure 6. VTSLM images of the $60 \mu\text{m} \times 60 \mu\text{m}$ void taken at the same temperature with different bias currents. (a) 0.1 mA (b) 1.0 mA (c) 5.0 mA. The resistance for each image is (a) 2.52Ω , (b) 2.52Ω and (c) 2.61Ω .

the resistance is almost same for each image. Figure 6(a) was biased with 0.1 mA, (b) with 1.0 mA and (c) with 5 mA. The resistance is (a) 2.52Ω , (b) 2.52Ω and (c) 2.61 , respectively. Since the values of the resistance are close together, these three images are similar. As seen in the figure, the image with 0.1 mA is fainter than other images because the maximum AC voltage response is low compared to (b) and (c). The maximum voltage response for each image was (a) $5.05 \times 10^{-7} \text{ V}$, (b) $2.22 \times 10^{-6} \text{ V}$, and (c) $1.25 \times 10^{-5} \text{ V}$. The amount of current applied has an effect on the magnitude of ac voltage response, but it doesn't change the shape of the image. With higher bias current, higher AC voltage response is obtained. Therefore, there is a strong correlation between the VTSLM images and the resistance of the sample.

VTSLM Images Using 2 Different Lasers

Figure 7 shows the VTSLM images taken using two different power of lasers: 5.2 mW and 20mW. The sample was biased with a current of 5 mA for all the images. Figure 7(a) was taken using 5.2 mW power of HeNe laser with the resistance of 1.010Ω and (b) was taken using 20 mW HeNe laser with 1.485Ω . The resistance of (a) and (b) are not exactly the same, but comparatively close to each other. Thus, they show similar images. Figure 7(c) and (d) have higher resistances than (a) and (b). The image (c) was taken using 5.2 mW laser with 4.580Ω and (d) was taken using 20 mW laser with 4.495Ω . As seen in the images, they are almost identical. The maximum voltage response for each image was (a) $1.63 \times 10^{-6} \text{ V}$ with 5.2 mW laser, (b) $5.13 \times 10^{-6} \text{ V}$ with 20 mW laser, (c) $2.31 \times 10^{-6} \text{ V}$ with 5.2 mW laser, and (d) $1.02 \times 10^{-5} \text{ V}$ with 20 mW laser. Therefore, the output power of the laser affects the magnitude of AC voltage response, but it does not change VTSLM images.

CONCLUSIONS

We have applied the VTSLM to study ac voltage response images of transport current distribution of a high temperature superconducting (HTS) film. The current distribution images

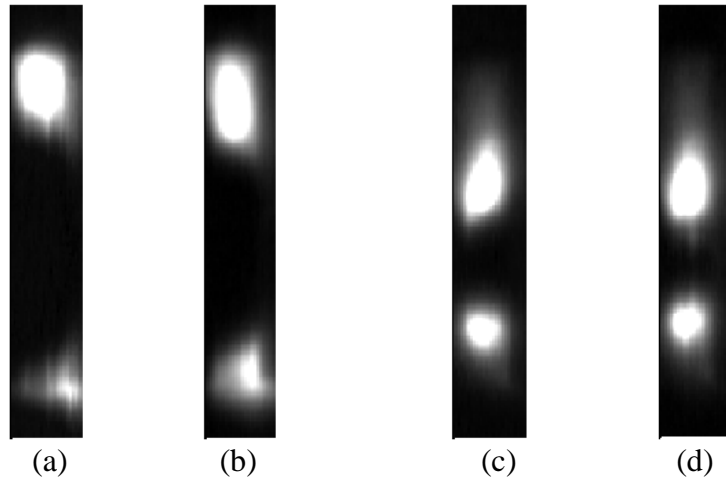


Figure 7. VTSLM images of the $10\ \mu\text{m} \times 10\ \mu\text{m}$ void taken using different power of lasers with a bias current of 5 mA. 5.2 mW power of HeNe laser was used for (a) and (c). 20 mW-laser was used for (b) and (d). The resistance is (a) $1.101\ \Omega$ (b) $1.485\ \Omega$ (c) $4.580\ \Omega$ (d) $4.495\ \Omega$.

in a $300\ \mu\text{m}$ -wide bridge show that there is a strong correlation between VTSLM images and the resistance of the sample. Also, the area with large δV shifts towards the end of the bridge with decreasing resistance. Further, VTSLM images taken below superconducting transition region show that the ends of the bridge become initially resistive near the critical current, I_c . Lastly, the amount of current less than the critical current, I_c , and the power of the laser have nothing to do with the VTSLM images. In this study it has been shown that the VTSLM is a unique and powerful technique to study the spatial distribution of superconducting properties and to identify the weaker superconducting areas.

Research supported by the Air Force Office of Scientific Research under contract No. F49620-01-1-0493.

REFERENCES

1. M. E. Gaevski, A. V. Bobyl, D. V. Shantsev, Y. M. Galperin, T. H. Johnsen, M. Baziljevich, H. Bratsberg, and S. F. Karmanenko, *Phys. Rev. B* **59**, 9655 (1999)
2. M. V. Indenbom, C. J. van der Beek, M. Konczykowski, and F. Holtzberg, *Phys. Rev. Lett.*, **1792** (2000).
3. J. Albrecht, Ch. Joose, R. Worthmann, A. Forkl, and H. Kronmuller, *Phys. Rev. B* **57**, 10332 (1998).
4. D. M. Feldmann, J. L. Reeves, A. A. Polynskii, A. Goyal, R. Feenstra, D. F. Lee, M. Paranthaman, D. M. Kroeger, D. K. Christen, S. E. Babcock, and D. C. Larbalestier, to be published in *IEEE Trans. Appl. Supercd.*
5. D. M. Feldmann, J. L. Reeves, A. A. Polynskii, G. Kozlowski, R. R. Biggers, R. M. Nekkanti, I. Maartense, M. Tomsic, P. Barnes, C. E. Oberly, T. L. Peterson, S. E. Babcock, and D. C. Larbalestier, *Appl. Phys. Lett.* **77**, 2906 (2000)
6. G. Karapetrov, V. Cambel, E. K. Kwok, R. Nikolova, G. W. Crabtree, H. Zheng, and B. W. Veal, *J., Appl. Phys.* **86**, 6282 (1999).